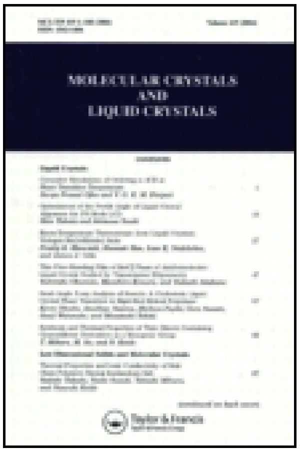

Molecular Crystals and Liquid Crystals Science and Technology. Section A. Molecular Crystals and Liquid Crystals
Publication details, including instructions for authors and subscription information:
http://www.tandfonline.com/loi/gmcl19

Switching of pixels in surface-stabilized ferroelectric liquid crystal cells

Th. Seitz [a], J. Stelzer [a] & H.-R. Trebin [a]
[a] Institut für Theoretische und Angewandte Physik Universität Stuttgart, Pfaffenwaldring 57, D-70550, Stuttgart, Germany

Version of record first published: 04 Oct 2006

Mol. Cryst. Liq. Cryst., 1997, Vol. 302, pp. 69–77
Reprints available directly from the publisher
Photocopying permitted by license only

Switching of pixels in surface-stabilized ferroelectric liquid crystal cells

Th. Seitz, J. Stelzer, and H.-R. Trebin
Institut für Theoretische und Angewandte Physik
Universität Stuttgart, Pfaffenwaldring 57, D-70550 Stuttgart, Germany

June 21, 1996

Abstract

Switching of pixels in surface-stabilized ferroelectric liquid crystal cells is studied. We have performed numerical calculations in two spatial dimensions on an adaptive grid to determine solutions for the scalar fields of the director twist angle and the electric potential. In the bulk we employ the full Frank-Oseen energy (i.e. no one-constant approximation) with the addition of electric terms represented by a uniaxial dielectric tensor and the spontaneous polarization. On the surface the director is anchored by a Rapini-Papoular potential. An idealized *bookshelf*-configuration with fixed tilt angle of the director is assumed. During both switching on and off disclination pairs are created on the surface. These disclinations form the ends of Bloch walls which bound the pixel. In the range of medium voltages after switching on an internal wall remains within the pixel which leads to an inhomogeneous director field and complicates switching off.

1 Introduction

Surface-stabilized ferroelectric liquid crystal (SSFLC) cells [1] allow fast switching by short pulses of an external voltage. In displays disclinations and domain walls are created during the switching process in between the pixels. In [2] we had discussed the motion of defects in SSFLC cells and had found that 360° walls are formed *within* the pixel. These internal walls affect the electro-optical properties of the display.

Here we are studying the processes of switching a pixel on and off in more detail and discussing the respective relaxation behaviour.

In our calculations we go beyond the one-constant approximation for the elastic energy and employ a uniaxial dielectric tensor. The electric potential U is calculated as well as the twist angle field ϕ, by simultaneous integration of the two governing differential equations on an adaptive grid.

2 Theory

We consider a SSFLC cell with a geometry as in Fig. 1. A smectic C^* liquid crystal is filled in between two parallel cover glasses at Cartesian coordinates $x = 0$ and $x = d$. The smectic layers run parallel to the x-y-plane (*bookshelf*-configuration). The tilt angle θ is taken to be constant, leaving a rotational motion on the tilt cone only. Thus the director $\vec{n}$ is completely described by the twist angle ϕ. We restrict ourselves to a two-dimensional geometry, i.e. all functions depend only on the x- and z-coordinates and are constant along the y-direction. There are two unknown quantities: the twist angle $\phi(x, z, t)$ and the electric potential $U(x, z, t)$.

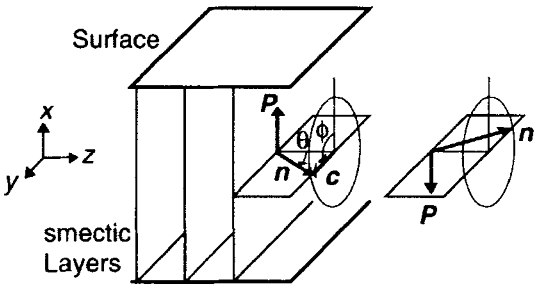

Figure 1: Geometry of the SSFLC-cell.

2.1 Material functions

To obtain the differential equations for these quantities, we make use of phenomenological material functions. The free energy density $\mathcal{F}$ consists of an elastic part in the form of the Frank-Oseen energy [4] and an electric part, which describes the interaction of the molecules with an electric field via induced and spontaneous polarizations [5]:

$$\begin{aligned} \mathcal{F}^B &= \frac{1}{2}k_{11}(\mathrm{div}\vec{n})^2 + \frac{1}{2}k_{22}(\vec{n}\cdot\mathrm{curl}\vec{n} - q_0)^2 \\ &+ \frac{1}{2}k_{33}(\vec{n}\times\mathrm{curl}\vec{n})^2 + \frac{1}{2}k_{24}\mathrm{div}(\vec{n}\mathrm{div}\vec{n} - \vec{n}\times\mathrm{curl}\vec{n}) \\ &- \frac{1}{2}\epsilon_0\,\mathrm{grad}U\cdot\underline{\underline{\epsilon}}\cdot\mathrm{grad}U + \mathrm{grad}U\cdot\vec{P}, \end{aligned} \tag{1}$$

where $\vec{n}$ denotes the director, U the electric potential and $\underline{\underline{\epsilon}}$ the dielectric tensor; k_{11}, k_{22}, k_{33} and k_{24} are the elastic constants of the liquid crystal; q_0 is the intrinsic twist due to a chiral dopant. The dielectric anisotropy is expressed by the uniaxial tensor $\underline{\underline{\epsilon}}$ [7]:

$$\underline{\underline{\epsilon}} = \frac{1}{3}\mathrm{trace}(\underline{\underline{\epsilon}})\underline{\underline{1}} + (\epsilon_{\|} - \epsilon_{\perp})(\vec{n}\otimes\vec{n} - \frac{1}{3}\underline{\underline{1}}), \tag{2}$$

with the eigenvector $\vec{n}$ belonging to the eigenvalue $\epsilon_{\|}$ and the degenerate eigenvalues $\epsilon_{\perp}$ belonging to all eigenvectors perpendicular to $\vec{n}$. Because of the missing inversion symmetry of the smectic C^* phase, the spontaneous polarization $\vec{P}$ stands perpendicular to the director $\vec{n}$ and is situated within the smectic layers [6]. We fulfill the geometrical constraints on $\vec{n}$ and $\vec{P}$ by expressing both vectors in spherical coordinates:

$$\vec{n} = \begin{pmatrix} \sin\theta\cos\phi \\ \sin\theta\sin\phi \\ \cos\theta \end{pmatrix}, \qquad \vec{P} = p_0\begin{pmatrix} \sin\phi \\ -\cos\phi \\ 0 \end{pmatrix}, \tag{3}$$

For the surface free energy we apply the Rapini-Papoular potential [8]:

$$\mathcal{F}^S = \frac{1}{2}c_\phi\sin^2(\phi - \phi_r). \tag{4}$$

The quantitity c_ϕ measures the anchoring strength, while ϕ_r determines the preferred director orientation on the surface. In the SSFLC cell $\phi_r = 90°$.

The total free energy per unit length of the cell in y-direction is given by

$$F = \int_0^d \int_0^b \mathcal{F}^B dx\, dz + \int_0^b \mathcal{F}^S dz. \tag{5}$$

2.2 Differential equations

By variation of the total free energy (5) nonlinear coupled partial differential equations are obtained for the twist angle ϕ and the electric potential U in the bulk and on the surface. In order to study switching processes we add a phenomenological viscous term. Inertial terms for the twist angle ϕ as well as time derivatives for the electric potential U may be neglected. The k_{24}-term is discarded. Thus we obtain the following dynamic equations:
bulk:

$$\begin{pmatrix} \gamma_1 \sin^2\theta \frac{\partial}{\partial t} + \sin^2\theta C_{ik}\partial_i\partial_k + \frac{1}{2}\sin^2\theta \frac{\partial C_{ik}}{\partial\phi}(\partial_i\phi)\partial_k & \frac{1}{2}\epsilon_0 \frac{\partial\epsilon_{ik}}{\partial\phi}(\partial_i U)\partial_k - \frac{\partial P_i}{\partial\phi}\partial_i \\ \frac{1}{2}\epsilon_0 \frac{\partial\epsilon_{ik}}{\partial\phi}(\partial_i U)\partial_k - \frac{\partial P_i}{\partial\phi}\partial_i & \epsilon_0\epsilon_{ik}\partial_i\partial_k + \frac{1}{2}\epsilon_0\frac{\partial\epsilon_{ik}}{\partial\phi}(\partial_i\phi)\partial_k \end{pmatrix} \begin{pmatrix} \phi \\ U \end{pmatrix} = \begin{pmatrix} 0 \\ 0 \end{pmatrix} \tag{6}$$

surface:

$$\alpha \sin^2\theta \frac{\partial\phi}{\partial t} + \frac{1}{2}c_\phi \sin 2(\phi - \phi_r) \pm (\sin^2\theta\, C_{xi}\partial_i\phi - Q_x) = 0 \tag{7}$$

The negative sign applies for the lower cover glass ($x = 0$), the positive sign for the upper one ($x = d$). γ_1 and α are the viscosities for rotational motion on the tilt cone in the bulk and on the surface, respectively. For the electric potential U we assume Dirichlet boundary conditions on the cover glasses. Along the z-direction we apply periodic boundaries. The first equation of the dynamic system (6) is parabolic, the second one is elliptic. The following abbreviations have been used:

$$\vec{Q}(\phi) = \underline{\underline{T}}^t_\phi \underline{\underline{T}}^t_\theta \begin{pmatrix} 0 \\ q_0 k_{22}\sin\theta \\ 0 \end{pmatrix},$$

$$\underline{\underline{C}}(\phi) = \underline{\underline{T}}^t_\phi \underline{\underline{T}}^t_\theta \operatorname{diag}(k_{11}, k_{22}, k_{33}) \underline{\underline{T}}_\theta \underline{\underline{T}}_\phi, \quad \underline{\underline{\epsilon}}(\phi) = \underline{\underline{T}}^t_\phi \underline{\underline{T}}^t_\theta \operatorname{diag}(\epsilon_\perp, \epsilon_\perp, \epsilon_\parallel) \underline{\underline{T}}_\theta \underline{\underline{T}}_\phi,$$

$$\underline{\underline{T}}_\phi = \begin{pmatrix} \sin\phi & -\cos\phi & 0 \\ \cos\phi & \sin\phi & 0 \\ 0 & 0 & 1 \end{pmatrix}, \quad \underline{\underline{T}}_\theta = \begin{pmatrix} 1 & 0 & 0 \\ 0 & \cos\theta & -\sin\theta \\ 0 & \sin\theta & \cos\theta \end{pmatrix}.$$

2.3 Numerical procedure (*cf.* [2])

We spatially discretize the differential equations on an adaptive grid by the finite difference method. For the time integration of the twist angle ϕ we use an explicit Euler method [10]. The static equation for the electric potential U is solved numerically by a multi-grid method [9] following each time step. The grid hierarchy is constructed adaptively at each time step before the integration is performed.

3 Numerical results and discussion

3.1 Visualization of the results

In the figures the twist angle is represented by the c-director, which is placed in the paper plane (the x-z-plane), although it actually lies in the x-y-plane. It is drawn only for the two grids lowest in the grid hierarchy. The cover glasses are on the top and bottom. The greyshaded background represents the twist angle. Halftoning limits the number of shades to about eighteen. Light grey corresponds to $\phi = 90°$ ($\vec{c}$-director points up), dark grey to $\phi = -90°$ ($\vec{c}$-director down). Regions with polarization UP or DOWN therefore are shaded in light or dark grey, whereas walls between them are shaded in medium grey tones.

3.2 Switching of pixels

For a pixel we assume a simple model of electrodes and boundary conditions on the surfaces at $x = 0$ and $x = d$. The central thirds of these surfaces are the electrodes of the pixel examined, where the electric potential is set to ± 10 V, respectively to switch the pixel on, and to ∓ 10 V to switch it off. The left and right thirds are electrodes of the neighbouring pixels. These are constantly set to zero potential. There is a small region between the electrodes, where the potential is interpolated linearly. It has to be kept in mind that the pixels examined have a much smaller width than a pixel of a typical LCD (about 17μm and 33μm *vs.* 200μm $\ldots 300\mu$m).

3.2.1 Switching a pixel on

The electric field is strongest where on each of the surfaces the voltage rises from zero of the neighbouring pixels to the full voltage of the central pixel. Disclinations are being formed there in pairs of opposite sign. Those with positive sign move towards the center of the switching electrode, those with negative sign remain at their positions (Fig. 2).

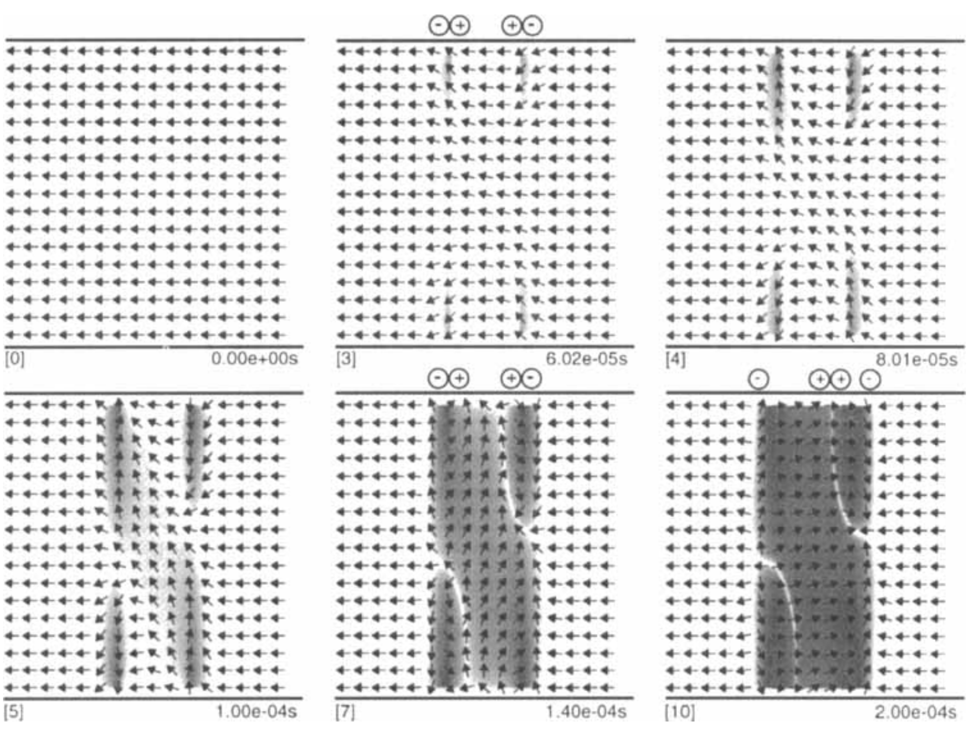

Figure 2: Switching a pixel on. An external voltage of 10 V is applied to the central thirds of the electrodes. The left and right thirds are set to zero potential. The circled + and − symbols exemplarily denote $+\frac{1}{2}$- and $-\frac{1}{2}$-disclinations, respectively.

The sense of the director rotation is initially governed by the induced polarization [2], subsequently by the spontaneous polarization. Repulsive elastic forces act between the positive surface disclinations. As a consequence these approach each other only up to a minimum distance, depending on the applied external voltage. Under further compression by a sufficiently strong electric field it is to be expected that the 360°-walls dissolve by means of an intermediary transition of their core into a smectic A phase, which allows the twist angle to relax by leaving the tilt cone. The $+1/2$-surface disclination pairs then are able to coalesce into $+1$-disclinations, one on each surface. Both then leave their surface and move towards the center of the bulk, where they deflect one another laterally. Each now forms together with the $-1/2$-surface disclinations above and below a twin Bloch wall, which bounds the pixel (this model for a domain wall has been proposed by Ouchi *et al.* [11]).

As our theoretical model does not account for phase transitions, we currently are not able to pursue such a scenario, though a crude approximation may be achieved by limiting the numerical algorithm to grids which just cannot resolve the 360°-walls. This is discussed below in section 3.4.

The $\pm\frac{1}{2}$-disclinations do not meet exactly in the center of the electrodes because the *uniform switching* process in the center of the cell acts asymetrically on the two disclinations.

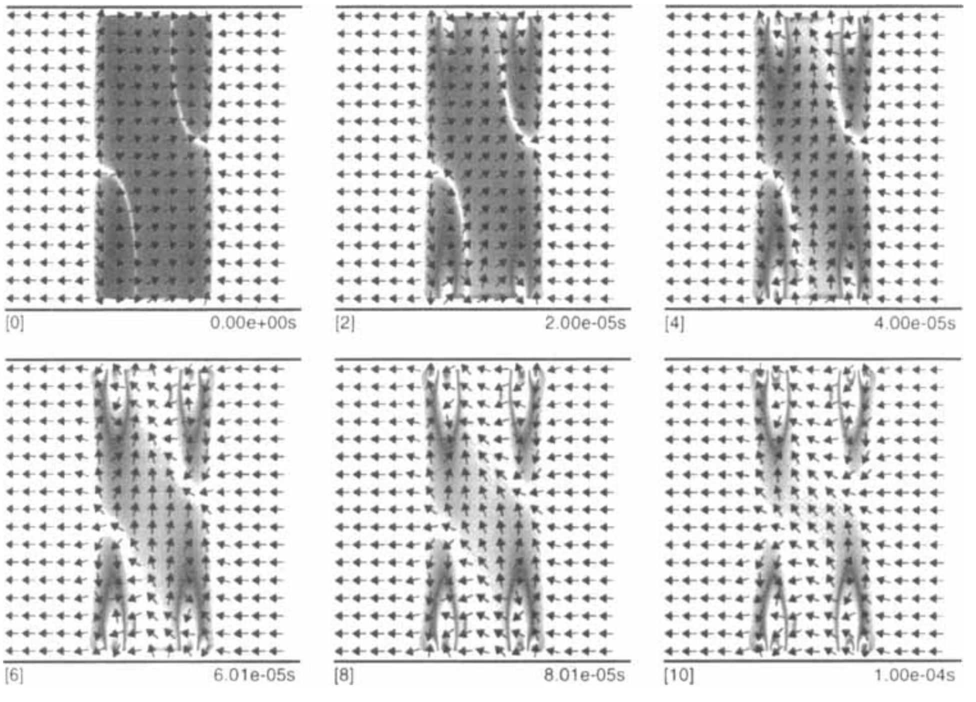

Figure 3: Switching the pixel off again. The external voltage is reversed. The simulation started with the last configuration shown in Fig. 2.

3.2.2 Switching a pixel off.

To switch the pixel off, a reversed voltage is applied to the central electrodes (cf. Fig. 3).

As in the process of switching on pairs of surface disclinations are generated. Again those of positive sign move towards the center of the surfaces. Compared to switching on the phase of the disclinations is changed by 180°. The new walls expand, while the old ones contract, until they meet and form 360°-walls. Then the switching off process is completed.

3.3 Relaxation

To check the bistability of a pixel and to study the dynamics of defects without the influence of an external field, we relaxed the sample after each switching process (*on* or *off*). Thereby we were motivated by observations of Pindak *et al.* [3] where 360°-walls disappeared either by retracting to the edge, if the wall ends in a point defect, or by the collapse of closed loops.

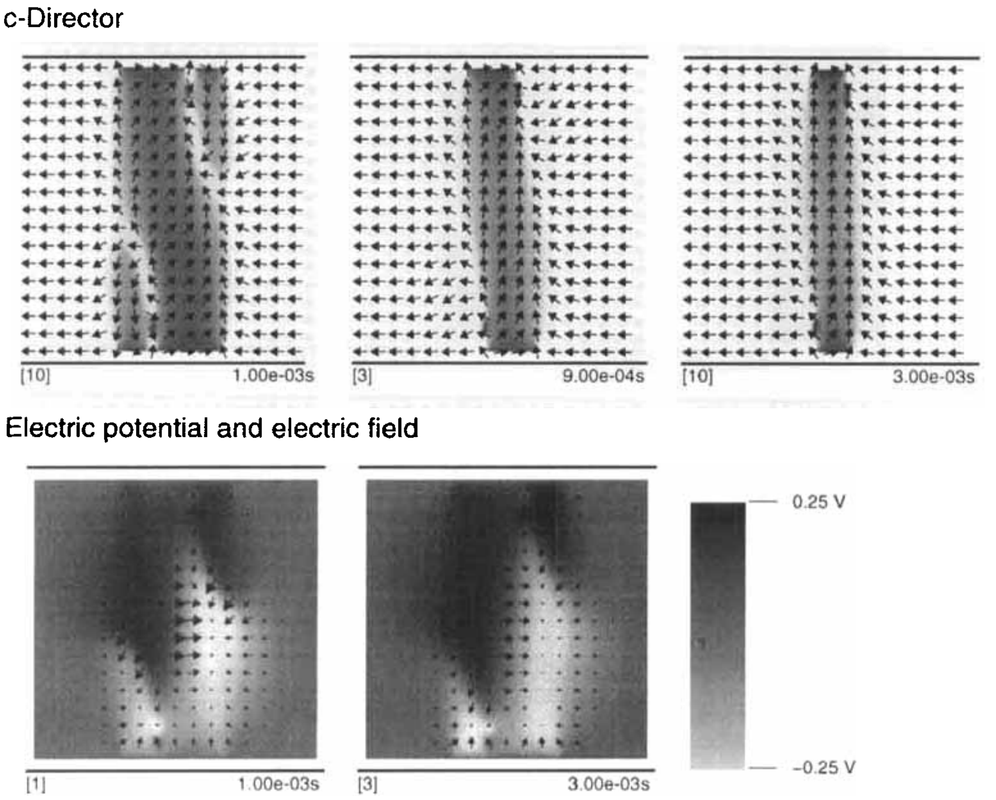

Figure 4: Relaxation of the switched pixel at zero voltage. The simulation started with the last configuration shown in Fig. 2.

3.3.1 Relaxation after switching on

As seen in Fig. 2 the 360°-walls branch into standard 180°-walls at the pixel boundary. The walls divide the pixel into three regions: a large region connecting the glass plates and two symmetrical small regions in the upper right and lower left. The large region is attached to both surfaces, whereas the small regions touch only one of them. In the course of the relaxation they retreat to this surface by collapse of the 180°-walls bounding them. (cf. Fig. 4).

The boundary of the large region is being smeared out during relaxation. Initially these effects cause an internal electric field due to the sponatenous polarization. As shown in Fig. 4 this field lies almost parallel to the glass plates and turns the c-director into an upright position. As the relaxation proceeds, the electric fields weakens and it is to be expected that the surface stabilization reorients the c-director in the *center of the cell* to the switched position $\phi = -90°$. Because the small regions vanish, the boundary of the large region is strongly curved. However, as the surface stabilization is only effective between opposite sections of the surface with equal orientation, the *boundaries of the pixel* appear fuzzy.

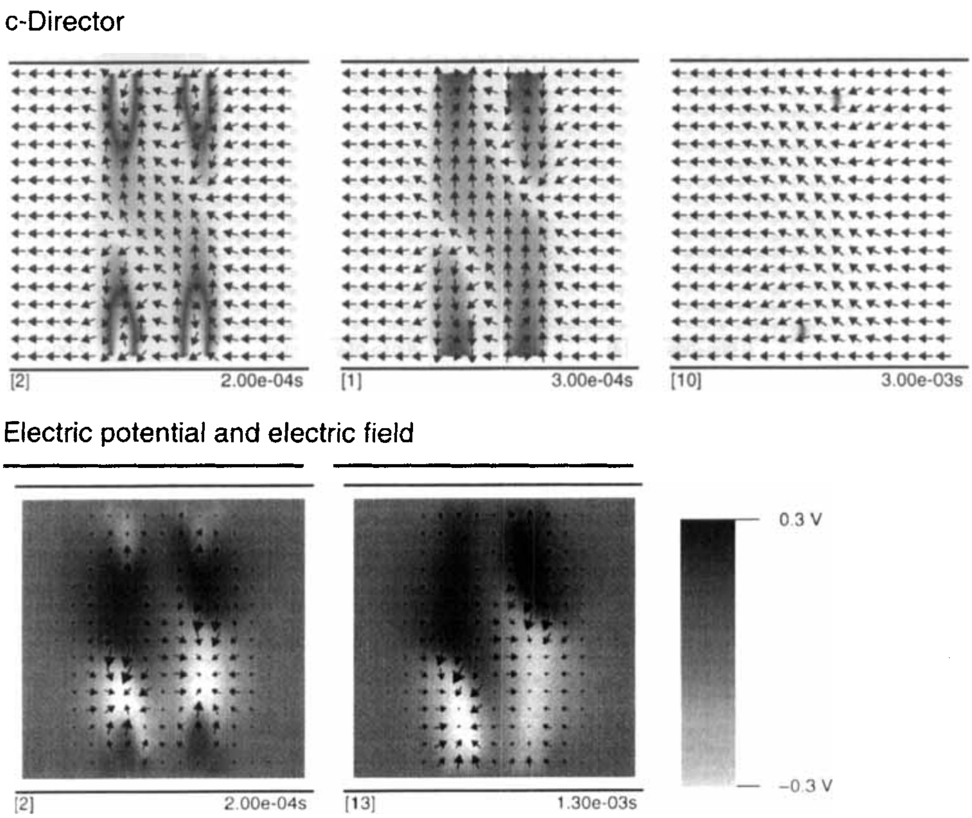

Figure 5: Relaxation at zero voltage after switching off. The simulation started with the last configuration shown in Fig. 3.

3.3.2 Relaxation after switching off

After switching the pixel off the walls form loops completed by sections of the surfaces and thus may collapse (cf. Fig. 5). Again, in the beginning of the relaxation process an internal electric field is generated almost parallel to the glass plates which tries to orient the c-director into an upright position. Because of the preceding process of switching off, though, the c-director on the surface points almost everywhere into the *off*-position. Upon weakening of the electric field, this position is stabilized in the bulk.

3.4 Pixel without internal walls

In this calculation the finest possible grid could not resolve the 360°-walls, thereby crudely simulating their vanishing due to a hypothetical phase transition to smectic A. The remaining Bloch walls meet in a +1 bulk disclination and form twin Bloch walls. As a consequence the process of switching off is greatly simplified, being the direct reversal of the process of switching on (cf. Fig. 6).

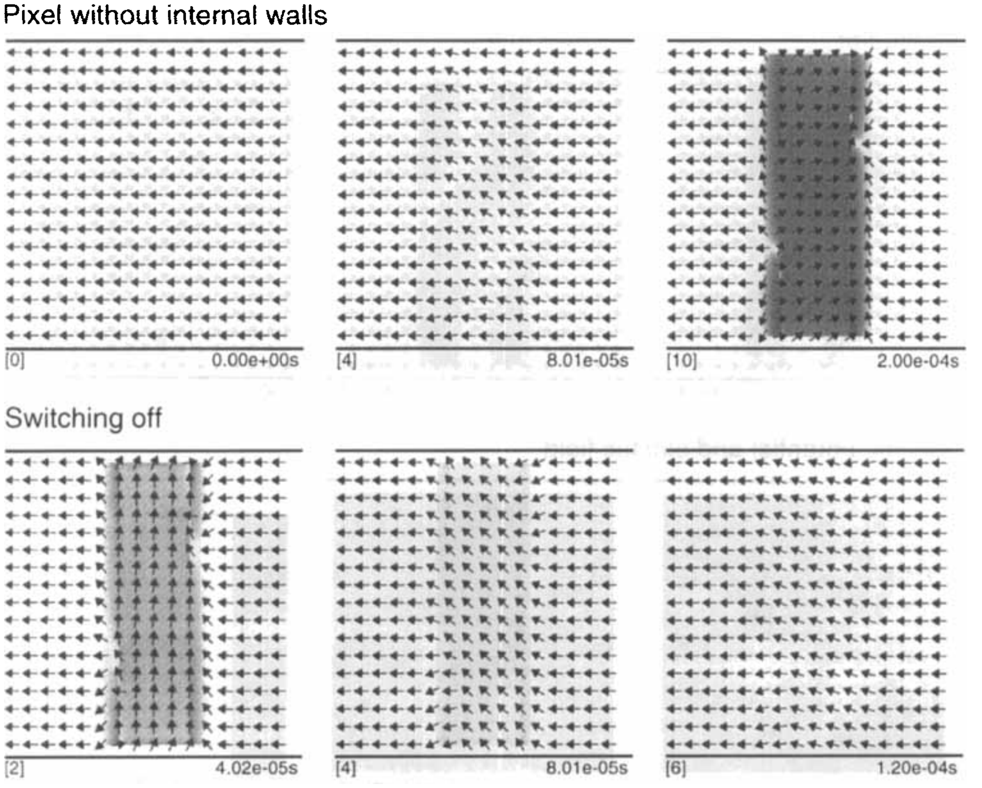

Figure 6: Pixel without internal walls (in this calculation due to numerical reasons as a crude simulation of a hypothetical phase transition). Switching off is greatly simplified, being the reversal of switching on.

4 Conclusion

The generation of internal 360°-walls has adverse effects on the electro-optical switching properties of SSFLC-displays. Their dissolution during switching to get twin Bloch walls would be desirable.

References

[1] N. A. Clark, S. T. Lagerwall, Appl. Phys. Lett. **36**, 899 (1980).

[2] Th. Seitz, J. Stelzer, H.-R. Trebin, J. Appl. Phys. *to be published in July 1996.*

[3] R. Pindak, C. Y. Young, R. B. Meyer, N.A. Clark, Phs. Rev. Lett. **45**, 1193 (1980)

[4] F. C. Frank, Faraday Soc. Disc. **25**, 19 (1958).

[5] More exactly one should denote $\mathcal{F}$ a Lagrangian density. It arises from a Legendre transform of the free energy density where the dielectric displacement is replaced by the electric field as in H. Gruler, T. J. Scheffer, G. Meier, Z. Naturforsch. **27a**, 966 (1972).

[6] R. B. Meyer, L. Liebert, L. Strzelecki, P. Keller, J. Phys. (Paris) Lett. **36**, L69 (1975)

[7] G. Vertogen and W. H. de Jeu, *Thermotropic Liquid Crystals*, Springer, Berlin, 1988.

[8] A. Rapini, M. Papoular, J. de Physique Coll. **30** C4, 54 (1969).

[9] W. Hackbusch, *Multi-Grid Methods and Applications*, Springer Verlag, Berlin, Heidelberg 1985.

[10] W.H. Press, S.A. Teukolsky, W.T. Vetterling, B.P. Flannery, *Numerical Recipes in C*, Cambridge University Press, 1992.

[11] Y. Ouchi, H. Takezoe, A. Fukuda, Jap. Jour. of Appl. Physics **26** No. 1, 1 (1987).